A Genetic Algorithm for the Topology Correction of Cortical Surfaces

Florent Ségonne[1,2], Eric Grimson[1], and Bruce Fischl[1,2]

[1]MIT C.S.A.I.L.
[2]Athinoula A. Martinos Center - MGH/NMR Center

Abstract. We propose a technique to accurately correct the spherical topology of cortical surfaces. We construct a mapping from the original surface onto the sphere to detect topological defects as minimal non-homeomorphic regions. A genetic algorithm corrects each defect by finding the maximum-a-posteriori retessellation in a Bayesian framework. During the genetic search, incorrect vertices are iteratively identified and eliminated, while the optimal retessellation is constructed. Applied to synthetic and real data, our method generates optimal topological corrections with only a few iterations.

1 Introduction

The human cerebral cortex is a highly folded ribbon of gray matter that lies inside the cerebrospinal fluid and outside the white matter of the brain. Locally, its intrinsic "unfolded" structure is that of a two-dimensional (2-D) sheet, which is several millimeter thick. The analysis of cortical data is greatly facilitated by the use of accurate 2-D models of the cortical sheet [1, 5], which alleviates most drawbacks of the three-dimensional embedding space (such as the underestimation of true cortical distances or the overestimation of cortical thicknesses). In the absence of pathology, each cortical hemisphere is a simply-connected 2-D sheet of neurons that carries the simple topology of a sphere. There has been extensive research dedicated to the extraction of accurate and topologically-correct models of the brain surface that allows for the establishment of a global 2-D coordinate system onto the cortical brain surface. However, because of its highly convoluted nature that results in most of its surface being buried within folds, noise, imaging artifacts, partial voluming effects and intensity inhomogeneities, the automatic extraction of accurate and topologically correct cortical surfaces is still a challenging problem.

Methods for producing topologically correct cortical models can be divided into two categories. Several approaches directly incorporate topological constraints into the segmentation process. A model, carrying the desired topology, is iteratively deformed onto the cortical surface while preserving its topology. To this end, active contours [3, 4, 2, 9, 19] and digital models [12, 15] have shown to be extremely useful. Unfortunately, the energy functionals driving the deformation are highly non-convex and the achievement of the desired final surface most

G.E. Christensen and M. Sonka (Eds.): IPMI 2005, LNCS 3565, pp. 393–405, 2005.

often requires an initialization of the model that is close to its final configuration. In addition, local topological constraints can easily lead to large geometric inaccuracies in the final cortical representation, which are difficult to correct.

Recently, new approaches have been developed to retrospectively correct the topology of an already segmented image. These techniques, which do not enforce any topological constraints into the segmentation process, can focus on more accurate models. Many segmentation techniques, using local intensity, prior probabilities, and/or geometric information without regard to topology, will be able to generate accurate cortical surfaces, with few topological inconsistencies.

Most methods assume that the topological defects in the segmentation are located at the thinnest parts of the volume and aim at correcting the topology by minimally modifying the volume or tessellation [17, 8, 18]. While these methods can be effective, most of them do not use any geometric or statistical information. Although they will often lead to accurate results, due to the accuracy of initial segmentations, topological corrections may not be optimal: additional information, such as the expected local curvature or the local intensity distribution, may lead to different corrections, i.e. hopefully comparable to the ones a trained operator would make.

Only a few techniques have been proposed to integrate additional information into the topology correction process. Using a digital framework, Kriegeskorte and Goeble [11] developed a technique that corrects each topological defect, located at the thinnest parts of the volume, by maximizing an empirical fitness function. More recently, another method to correct the topology of sub-cortical structures has been proposed but has not yet been applied to the reconstruction of cortical surfaces [16]. Unfortunately, digital approaches fail to integrate geometric information into the topology correction process.

In previous work, Fischl et al. [7] proposed an automated procedure to locate topological defects by homeomorphically mapping the initial triangulation onto a sphere. Topological defects are identified as regions in which the homeomorphic mapping is broken and a greedy algorithm is used to retessellate incorrect patches, constraining the topology on the sphere $\mathbb{S}$ while preserving geometric accuracy by a maximum likelihood optimization. In this approach, all possible edges in a defective region are ordered using some measure, then each edge is sequentially added to the existing tessellation if and only if it does not intersect any of the existing or previously added edges.

Although this approach can result in reasonable surfaces in many cases, it is worth noting that the information necessary to evaluate the "goodness" of an edge does not exist in isolation, but only as a function of the tessellation of which the edge is a part. This is a critical point, as it implies that a greedy algorithm cannot in general achieve geometrically accurate surfaces, as the necessary information does not exist at the time that the edge ordering is constructed. Another subtle point to be noted is that every vertex in the original defect, even those present due to segmentation inaccuracies, will be present in the final retessellation, resulting in extremely jagged patches that only a strong smoothing could correct. As a consequence, the final configuration will approximately correspond

to an average of all vertex positions in the original configuration. Finally, we note that, even though the final intrinsic topology will be the correct one (the one of a sphere, corresponding to an Euler number $\mathcal{X} = 2$ [1]), the proposed method does not guarantee that the final surface will not self-intersect.

In this paper, we propose a technique that directly extends the approach taken by Fischl et al. in [7], addressing most of its limitations. We focus on the retessellation problem and introduce a genetic algorithm to explore the space of possible surface retessellations and to select an optimal configuration. During the search, incorrect vertices are iteratively identified and eliminated from the tessellation.

2 Methods

In order to extend the greedy retessellation developed in [7], we propose to take a somewhat different approach, and evaluate the goodness of fit of the entire retessellation, not of individual edges.

Our method proceeds as follow:

1) Generate a mapping from the original cortical surface onto the sphere that is maximally homeomorphic. Each topological defect is identified as a set of overlapping triangles.
2) Discard the tessellation in each defect and generate an optimal retessellation using a genetic algorithm to search the space of potential retessellations.

2.1 Identification of Topological Defects

The first step is identical to the approach developed by Fischl et al. in [7]. Briefly, the identification of topological defects begins with the inflation and projection of the cortical surface $\mathcal{C}$ onto a sphere $\mathcal{S}$. Next, we generate a maximally homeomorphic mapping $\mathcal{M} : \mathcal{C} \rightarrow \mathcal{S}$ by minimizing an energy functional that directly penalizes regions in which the determinant of the Jacobian matrix of $\mathcal{M}$ becomes zero or negative (non-homeomorphic regions). More specifically, noting that the Jacobian yields a measure of the deformation of an oriented area element under $\mathcal{M}$, the energy functional $E_{\mathcal{M}}$ limits the penalization of compression primarily to negative semi-definite regions. If the initial area on the folded surface of the i^{th} face is A_i^0, and the area on the spherical surface $\mathcal{S}$ at time t of the numerical integration is A_i^t, then the energy functional is given by:

$$E_{\mathcal{M}} = \sum_{i=0}^{F} \log(\frac{1 + e^{kR_i}}{k}) - R_i \ , \ R_i = \frac{A_i^t}{A_i^0}.$$

[1] The Euler number of a surface is a topological invariant. For a tessellation, it can be easily computed as: $\mathcal{X} = \#vertices - \#edges + \#faces$. The Euler number of a sphere is $\mathcal{X} = 2$.

The resulting mapping - from the initial tessellation to the sphere - is maximally homeomorphic. Multivalued regions, containing overlapping triangles, constitute topological defects where the homeomorphic mapping is broken. $\mathcal{M}$ associates at each vertex v of the initial cortical surface $\mathcal{C}$ a vertex $v_S = \mathcal{M}(v)$ on the sphere $\mathcal{S}$. Vertices with spherical coordinates that intersect a set of overlapping triangles are marked as defective and topological defects are identified as connected sets of defective vertices (we refer to [7] for more details).

2.2 Definition of the Retessellation Problem

Once a topological defect has been identified, its tessellation is discarded. The retessellation problem can then be stated as follows.

> *Given a set of defective vertices, each of which has been assigned a spherical location by the quasi-homeomorphic mapping $\mathcal{M}$, find the vertices that should be kept in the defect and the set of edges connecting them, so that an energy functional, measuring the goodness of the retessellation, is maximized.*

Topological inconsistencies, which are resulting from mislabeled voxels in the segmentation process, generate tessellations that include incorrect vertices. These vertices should be identified and discarded from the final solution. A potential topological correction of the defect corresponds to the generation of a new tessellation such that no edge intersection occurs in the spherical surface. Many such tessellations exist [2], and one would like to select an optimal solution that maximizes the goodness of fit of the retessellation.

We evaluate the fitness of a corrected region with the maximum-a-posteriori estimate of the retessellation, given geometric information about the observed surface, and the underlying MRI values. The numerical technique we propose to explore in the maximization of the fitness function is a genetic algorithm or GA (for a good introduction see [14]). The GA is an appropriate choice for this type of problem as the space to be searched is potentially quite large (the defects can contain upwards of 300,000 candidate edges), and there is no easy way to compute gradient information. More importantly, we define a set of genetic operations used to propagate information from one generation to the next that correspond to 'relevant' surface operations.

2.3 A Genetic Algorithm for the Surface Retessellation

Genetic Algorithms were developed by John Holland in the 1960s as a means of importing the mechanisms of natural adaptation into computer algorithms and numerical optimization [10]. In genetic algorithms, a candidate solution to a problem is typically called a chromosome, and the evolutionary viability of each chromosome is given by a fitness function. Typically, genetic algorithms are defined by different operators: Selection, Crossover and Mutation.

[2] For a defect composed of n vertices, the number of potential edges is $N = n(n-1)/2$, leading to a space of size $O(2^N)$.

In the next paragraphs, we explain the role of these operators in detail and specify how their definition is meaningfully tailored to the current problem.

A - Representation and Retessellation: perhaps the most important decision in the construction of a GA is the choice of representation for the underlying problem. Here we have a number of constraints that must be satisfied that lead to the representation we use. These essentially amount to the requirement that every potential edge be represented exactly once in an ordering for the retessellation. This guarantees that the retessellation will result in the proper topology [7]. Thus the representation we choose is an edge ordering, represented by a permutation of N integers. The retessellation procedure then simply involves adding edges in the order specified by the permutation.

Such a procedure will generate retessellated patches that include all vertices present in the defect, resulting in irregular jagged surfaces. In order to alleviate this problem, we directly encode the vertex selection into the representation. Given an edge ordering, we construct the corresponding tessellation and assign to each vertex an arrival number based on the order in which they were added. Next, we discard all the vertices that were added after all of its neighbors, i.e. vertices with lower arrival numbers. This way, edges added first in the retessellation will force their bordering vertices to be included in the final retessellation. The edges added last, which most often generate the surface irregularities, will consequently be discarded.

B - Selection of the Initial Population: the selection of the initial population is particularly significant for the considered problem. The space to be searched is potentially quite large and the selection of a "good" initial population can drastically improve convergence of the algorithm. Topological defects are constituted of sets of overlapping triangles. The intersecting edges on the sphere $\mathcal{S}$ correspond to different topological paths in the original cortical surface $\mathcal{C}$. In order to generate an initial population with a large variance, i.e. composed of individuals with large *shape* differences, we first group the non-overlapping edges into different clusters. Using the spherical quasi-homeomorphic mapping M, intersecting edges are iteratively segmented into different clusters. Next, these clusters are used to select the initial population of chromosomes. We say that a chromosome is generated from a cluster C_i, if the first edges (in the ordering) constituting this chromosome comes from C_i. Consequently, chromosomes generated from different clusters will have different shapes, hopefully leading to an initial population with a large variance. Figure 1 provides a few examples of initially selected chromosomes in the case of a simple topological defect.

C - Mutation and Crossover: the two most important operations used in GAs are mutation and crossover. Mutation involves the random modification of a part of the code of an "individual" in the population and crossover the exchange of a part of the code of an "individual" with another one in the population. We define these operations in order to accommodate the nature of the current problem. Intersecting edges represent choice between different surface configurations. In the following section, we note I_i the set of edges intersecting the edge e_i: $I_i =$

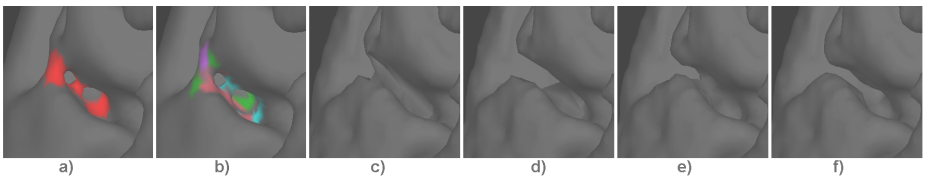

Fig. 1. a) Example of a topological defect containing 2 handles and constituted of 183 defective vertices. b) Result of the clustering of the non-intersecting edges into 5 segments. c-e) These candidate retessellations represent different configurations of the initial population generated using the edge clustering. f) The optimal solution generated by our genetic approach in 15 generations after 4 mutations and 8 crossovers

$\{e_j | \text{int}(e_i, e_j) = 1\}$, where $\text{int}(e_i, e_j)$ is the intersection operator, and returns 1 if edge e_i intersects edge e_j, and 0 otherwise.

For mutation, we perform the following operation for each possible edge in the tessellation:

1) Draw a random number r from $U_{\mathbb{R}}(0, 1)$, the uniform distribution on the real numbers between 0 and 1.
2) If $r > p_{mut}$ then continue with the next edge.
3) Draw a random number k from $U_{\mathbb{N}}(1, \#I_i)$, the uniform distribution on the natural numbers between 1 and $\#I_i$.
4) Exchange the positions of e_i and e_j, where e_j is the k^{th} entry in the set I_i.

This procedure will allow the selective exploration of the different retessellations represented by different members of I_i, thus reducing the size of the effective search space.

The crossover operator we define is the random combination of permutations. Some care must be taken here to insure that every edge is represented exactly one time. Towards that end, the crossover operator will add a random number of edges from each parent retessellation, only if that edge has not been added. The crossover operator will randomly select one of the permutations to draw from first, then copy a random number of edges from it to the "offspring" retessellation. For each edge, we draw a random number r from $U_{\mathbb{R}}(0, 1)$, and stop copying edges if $r < 1/2$. Next, a random number of edges will be copied from the second parent, if they are not already represented in the offspring. This procedure will continue until every edge is represented.

It is important to note that the previously defined genetic operations carry meaningful geometric operations. Mutation, which randomly swaps the ordering of intersecting edges, corresponds to local jumps from one configuration to another one. The crossover operation naturally combines different parts of the code from the two candidate tessellations, generating a configuration that often expresses distinct local surface properties of both parents. In addition, since the edge ordering naturally encodes which vertices are discarded (the vertices included last being discarded), the crossover operation, which iteratively combines two edge orderings, most often generates offspring chromosomes that preserve

the best geometric characteristics of the parents (most likely, the same vertices will be discarded).

D - Fitness and Likelihood Functions: we use some prior knowledge about the cortex to define the fitness function. A cortical surface is a smooth manifold $\mathcal{C}$ that partitions the embedding space into an inside part, composed of white matter, and an outside part, composed of gray matter. We characterize the goodness of a retessellation by measuring two of its properties:

(1) The smoothness of the resulting surface,
(2) the MRI values I inside and outside the surface.

Formally, the posterior probability of the i^{th} retessellation T_i is given by:

$$p(T_i|\mathcal{C}, I) \propto p(I|\mathcal{C}, T_i)p(T_i|\mathcal{C}).$$

The likelihood term $p(I|\mathcal{C}, T_i)$ encodes information about the MRI intensities inside and outside the surface. Each retessellated patch, being topologically correct, separates the underlying MRI volume into two distinct components [3], an inside part $\mathcal{C}^-$ and an outside part $\mathcal{C}^+$. An acceptable candidate solution should generates a space partition with most of its inside and outside voxels corresponding to white and gray matter voxels respectively. In order to estimate the likelihood $p(I|\mathcal{C}, T_i)$, we assume that the noise is spatially independent. This probability can be rewritten:

$$p(I|\mathcal{C}, T_i) = \underbrace{\prod_{x\in\mathcal{C}^-} p_w(I(x)|\mathcal{C}, T_i) \prod_{x\in\mathcal{C}^+} p_g(I(x)|\mathcal{C}, T_i)}_{\text{volume-based information}} \underbrace{\prod_{v=1}^{V_i} p(g_i(v), w_i(v)|\mathcal{C}, T_i)}_{\text{surface-based information}},$$

$p_w(I(x)|\mathcal{C}, T_i)$ and $p_g(I(x)|\mathcal{C}, T_i)$ are the likelihood of intensity values at location x in the volume inside and outside the tessellation respectively, $p(g_i(v), w_i(v)|\mathcal{C}, T_i)$ is the joint likelihood of intensity values inside and outside the tessellation at vertex v in tessellation T_i.

Geometric information can be incorporated via $p(T_i|\mathcal{C})$, which represents priors on the possible retessellation. For example, $p(T_i|\mathcal{C})$ could have the form:

$$p(T_i|\mathcal{C}) = \prod_{v=1}^{V_i} p(\kappa_1(v), \kappa_2(v)|\mathcal{C}),$$

where κ_1 and κ_2 are the two principal curvatures of the surface, computed at vertex v.

Given that the vast majority of the surface is in general not defective, we fortunately have ample amounts of data with which to estimate the correct forms

[3] We use the angle weighted pseudo-normal algorithm to compute the signed distance of the tessellation. The voxel grid is partitioned into inside negative values and outside positive values

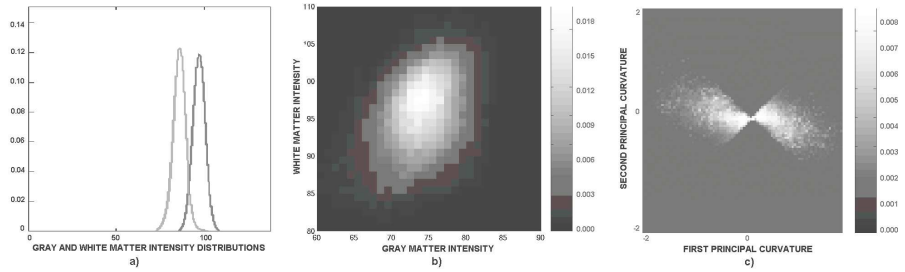

Fig. 2. a) Example of the gray and white matter distributions estimated locally from a given a topological defect. b) Joint distribution of gray and white matter given the surface computed using the non-defective portion of the gray/white boundary representation of a single subject. The gray and white matter intensity are two correlated variables, as indicated by the diagonal structure of the joint distribution. c) Joint distribution of two principal curvatures of the surface

of the distributions $p(T_i|\mathcal{C})$, $p_g(I(x)|\mathcal{C}, T_i)$, $p_w(I(x)|\mathcal{C}, T_i)$ and $p(g_i, w_i|\mathcal{C}, T_i)$. In particular, the single tissue distributions $p_g(I(x)|\mathcal{C}, T_i)$ and $p_w(I(x)|\mathcal{C}, T_i)$ are locally estimated around each topological defect in a region that excludes the defect itself (we exclude all voxels that intersect one of the N potential edges). This makes the resulting procedure completely adaptive and self-contained, in the sense that no assumptions need to be made about the contrast of the underlying MRI image(s), and no training or parametric forms are required for $p(T_i|\mathcal{C})$. An example of the estimation of $p(g_i, w_i|\mathcal{C}, T_i)$ and $p(T_i|\mathcal{C})$ is given in Fig. 2. Image b) shows the joint distribution of gray and white matter given the surface computed using the non-defective portion of the gray/white boundary representation of a single subject. Note the diagonal character of the distribution, indicating that the intensities are mutually dependent - brighter white matter typically means brighter gray matter due to factors such as bias fields induced by RF inhomogeneities and coil sensitivity profiles, as well as intrinsic tissue variability. One possible form of the priors on the tessellation is given in Fig. 2c, which shows the joint distribution of the two principal curvatures κ_1 (green) and κ_2 (red) computed over the non defective portion of a single surface. It is important to note in this context that all these distributions can only be applied after a candidate retessellation has been completed, as the gray/white joint density requires surface normals, gray and white intensity distributions necessitate the underlying MRI volume to be partitioned in two separate components and the principal curvatures require the calculation of the second fundamental form, all of which are properties of the surface, not of individual edges.

E - Iterative Elimination of Vertices: During the genetic search, some vertices will be consistently discarded from the best patches. These vertices, which are the ones that were erroneously kept in the initial cortical tessellation, should be identified and eliminated from the final tessellation. To this end, we introduce in our genetic search, an elimination operator, which selectively eliminates the worst vertices from the defect. The elimination step operates as follow: after

every few iterations, we eliminate the vertices that were consistently discarded from the best candidate patches.

The proposed approach is implemented with the following parameters. The initial population size is chosen depending on the number of defective vertices. The retessellation process is quadratic in the number of vertices contained within the convex hull of each defect. Typical defect contains on the order of 100 vertices for a population size of 20 candidate retessellations. At each step of the genetic search, a new population is generated from selected chromosomes based on their fitness. Given a population of individuals, the top one third is selected to form the elite group. These chromosomes are kept for the next generations. The worst individuals, corresponding to the bottom one third, are replaced with mutated copies of the best. Finally, the remaining ones are generated from crossover operations from parents iteratively chosen from the elite population. The mutation rate p_{mut} is experimentally chosen to be 10%. The algorithm stops when no new best candidate has been found for the past 10 generations. For a typical topological defect of size 100 vertices, the algorithm usually converges in less than 50 generations, which corresponds to a computational time of approximately 10 minutes on a 1-G-Hz Pentium IV. An optimal configuration is usually the result of approximately 30 genetic operations, 80% of which are crossovers and 20% mutations. The elimination operator is applied every 5 generations. The number of discarded vertices depends on the topological defect. In some cases, more than 40% will be eliminated.

3 Results and Discussion

Before reporting results of the proposed approach on synthetic and real datasets, we measure the goodness of our method relatively to a random search algorithm. This is to verify that our approach actually improves the speed of convergence and that the genetic operations allow the generation of superior candidate retessellations.

Genetic versus Random Search: we compared our approach with a random search algorithm, in which random permutations of the edge ordering were iteratively generated. The graphs in Fig. 3 illustrate the strength of our approach on a real data example. The topological defect is shown in Fig. 1a. For each method, the first candidate tessellation corresponded to the solution generated by the greedy approach proposed in [7] with its vertices added last being discarded (see sect 2.3.A). Compared to a random search, the genetic search converges much faster (at least, second order magnitude). The genetic algorithm boosts the overall fitness of the population by keeping the best representations at each generation and producing new candidates using the elite population. In a few generations composed of a small number of chromosomes (20 chromosomes per generation in this example), the genetic search is able to produce new optimal retessellations (see Fig. 1f).

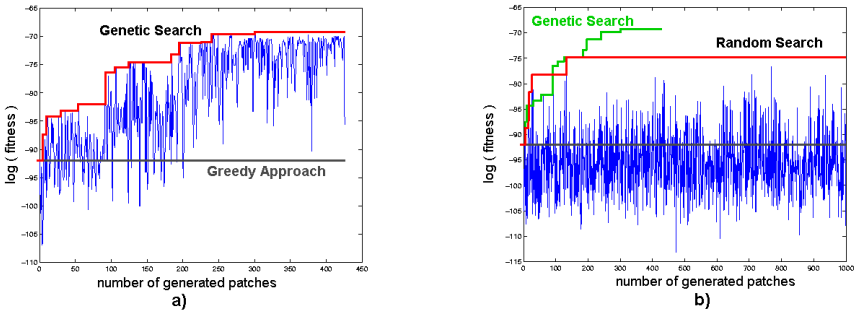

Fig. 3. a) Evolution of the log of the fitness function during the genetic search. b) Evolution of the log fitness function during a random search. Note how the genetic search iteratively improves the average fitness of each generated chromosome, which, as a consequence, will be able to generate new optimal chromosomes. On the other hand, random retessellation rarely generates new optimal patches. In this defect, which was constituted of 183 vertices, even after 50000 random draw, the fitness function of the best randomly generated chromosome was still 5 order of magnitude below the best GA chromosome (generated as the 300^{th} offspring during the 15^{th} generation)

Application to Synthetic Data and Real Data: in order to validate the proposed method, we first generated surfaces containing simple topological defects (handles, holes). These data were used to explore the performance of the algorithm relatively to typical topological defects. The underlying MRI volumes were generated by adding white noise to the expected tissue intensities : gray and white intensity values were drawn from Gaussian distributions $G(\mu_g = 90, \sigma_g = 5.0)$ and $G(\mu_w = 110, \sigma_w = 5.0)$ respectively. Figure 4, top row, illustrates the behavior of the algorithm relatively to different MRI volumes, when the same topological defect has to be corrected (left: a simple handle). We note that traditional active contour models could not have generated the same results due to the amount of noise in the images and the presence of large local minima in the energy functional.

We have applied our proposed approach on 35 real images. The dataset was composed of MRI volumes of different qualities, from different populations. Results were evaluated by an expert to assess the correctness of the final corrections. The algorithm was able to generate correct solutions that the initial greedy approach [7] failed to produce. Methods that do not integrate statistical and geometric information will often fail to produce solutions comparable to the ones a trained operator would make. This is illustrated in Fig. 4, bottom, where valid solutions do not always correspond to minimal corrections (i.e. cutting the handle in the two examples of Fig. 4). Only general approaches that integrate additional information can lead to correct solutions. An average cortical surface contains on the order of 50 topological defects, most of which are relatively small. A full brain is corrected in approximately 2 hours on a 1GHz PII machine. The average Hausdorff distance computed for each defect in between automatically and manually corrected surfaces is less than $0.2mm$.

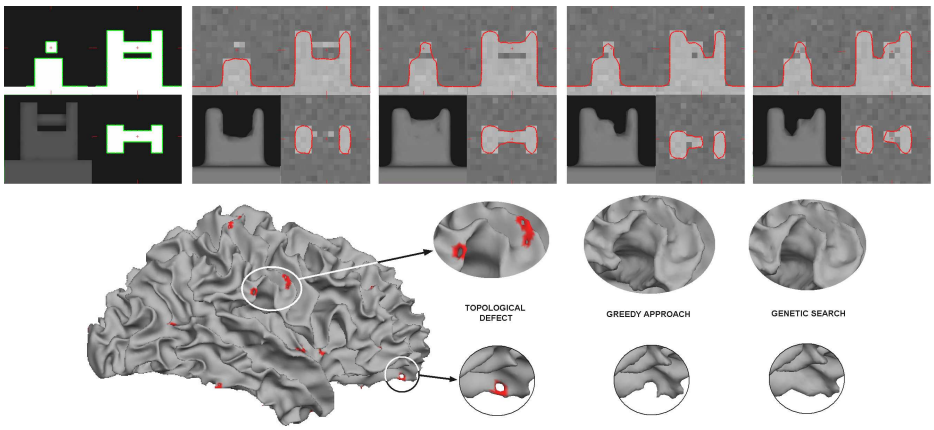

Fig. 4. Top row) Results of our proposed approach on different phantom examples. The same topological defect (left: a small handle constituted of about 100 vertices) is corrected using different underlying MRI volumes. In each case, our approach generated an optimal configuration corresponding to the expected solution. Bottom row) Topology correction of a cortical representation. The initial surface was constituted of 30 defects (Euler number $\chi = -58$). Compared to the greedy approach of Fischl et al. [7], which failed to find the correct solutions in many defects, our approach was able to generate valid solutions. This is illustrated on two examples, in which valid topological solutions do not correspond to minimal corrections

We note that the proposed method does not directly prevent the final surface from self-intersecting. Self-intersecting configurations typically have low fitness values and are naturally discarded during the genetic search. The self-intersecting constraint could be directly integrated into the retessellation process, but would drastically slow down the proposed approach. In our experience, final corrected representations rarely intersect (less than one in ten thousand faces, which corresponds to approximately 1 defect per brain). In order to ensure that the solution generates a valid manifold, we retrospectively check that the final retessellation does not self-intersect. In the case of self-intersection, we re-apply the genetic algorithm with the additional constraint of only generating valid candidate patches. Self-intersecting patches are identified and discarded from the population.

4 Conclusion and Future Work

We have proposed an automated method to accurately correct the topology of cortical representations. Our approach integrates statistical and geometric information to select the optimal correction for each defect. In particular, we have developed a genetic algorithm that is specifically adapted to the retessellation problem. Iterative genetic operations generate candidate tessellations that are selected for reproduction based on their goodness of fit. The fitness of a retes-

sellation is measured by the smoothness of the resulting surface and the local MRI intensity profile inside and outside the surface. The resulting procedure is completely adaptative and self-contained. During the search, defective vertices are identified and discarded while the optimal retessellation is constructed.

Given a quasi-homeomorphic mapping from the initial cortical surface onto the sphere, our method will be able to generate optimal solutions. For each defect, the space to be searched (i.e. the edge ordering) is dependent on the spherical location of the defective vertices. Some configurations of the quasi-homeomorphic mapping could lead to optimal but incorrect retessellations. In future work, we plan to address this limitation by directly integrating the generation of the homeomorphic mapping into the correction process.

References

1. A. M. Dale and M. Sereno, "Improved localization of cortical activity by combining EEG and MEG with MRI cortical surface reconstruction: A linear approach," J. Cogn. Neurosci., vol. 5, no.2, pp.162-176, 1993.
2. A. M. Dale, B. Fischl, and M. I. Sereno, "Cortical surface-based analysis I: Segmentation and surface reconstruction," NeuroImage, vol.9, pp. 179-294, 1999.
3. C. Davatzikos, and R.N. Bryan, "Using a Deformable Surface Model to Obtain a Shape Representation of the Cortex". IEEE T.M.I., 1996. 15: p. 785-795.
4. D. MacDonald, N. Kabani, D. Avis, and A. C. Evens, "Automated 3D extraction of inner and outer surfaces of cerebral cortex from MRI," NeuroImage, vol.12, pp. 340-356, 2000.
5. D. C. van Essen, and H. Drury, "Structural and functional analyses of human cerebral cortex using a surface-based atlas," Journal of Neuroscience, vol.17, no.18, pp7079-7102, 1997.
6. B. Fischl, and M. I. Sereno, and A. M. Dale, "Cortical surface-based analysis II: Inflation, flattening, and a surface-based coordinate system," NeuroImage, vol.9, pp. 195-207, 1999.
7. B. Fischl, A. Liu, and A. M. Dale, "Automated manifold surgery: Constructing geometrically accurate and topologically correct models of the human cerebral cortex," IEEE T.M.I., vol. 20, pp. 70-80, 2001.
8. X. Han, C. Xu, U. Braga-Neto, and J. L. Prince, "Topology correction in brain cortex segmentation using a multiscale, graph-based approach," IEEE T.M.I., vol. 21(2): 109–121, 2002.
9. X. Han, C. Xu, D. Tosun, and J. L. Prince, "Cortical Surface Reconstruction Using a Topology Preserving Geometric Deformable Model," MMBIA, Kauai, Hawaii, Dec. 2001, pp. 213-220.
10. Holland, J.H., "Adaptation in Natural and Artificial Systems," 1975, Ann Arbor: University of Michigan Press.
11. N. Kriegeskorte and R. Goeble, "An efficient algorithm for topologically segmentation of the cortical sheet in anatomical mr volumes. NeuroImage, vol. 14, pp. 329-346, 2001.
12. J.-F. Mangin, V. Frouin, I. Bloch, J. Regis, and J. Lopez-Krahe, "From 3D magnetic resonance images to structural representations of the cortex topography using topology preserving deformations," Journal of Mathematical Imaging and Vision, vol. 5, pp.297-318, 1995.

13. T. McInerney and D. Terzopoulos, "Deformable models in medical image analysis: A survey," Medical Image Analysis, vol.1, no.2, pp.91-108,1996.
14. M. Mitchell, "An introduction to genetic algorithms," MIT Press.
15. F. Poupon and J.-F. Mangin and D. Hasboun and C. Poupon and I. Magnin and V. Frouin, "Multi-object Deformable Templates Dedicated to the Segmentation of Brain Deep Structures", LNCS 1496, pp. 1134-1143, 1998.
16. F. Ségonne, B. Fischl, and E. Grimson, "Topology correction of Subcortical Structures," MICCAI 2003, LNCS 2879, pp.695-702.
17. D. W. Shattuck and R. Leahy, "Automated Graph-Based Analysis and Correction of Cortical Volume Topology," NeuroImage, vol. 14, pp. 329-346, 2001.
18. I. Guskov and Z. Wood, "Topological noise removal," GI 2001 proceedings, pp. 19-26, 2001.
19. X. Zeng, L. H. Staib, R. T. Schultz, and J. S. Duncan, "Segmentation and measurement of the cortex from 3D MR images using coupled surfaces propagation," IEEE T.M.I., vol. 18, pp. 100-111, 1999.